LASER INTERFEROMETER GRAVITATIONAL WAVE OBSERVATORY
- LIGO -
CALIFORNIA INSTITUTE OF TECHNOLOGY
MASSACHUSETTS INSTITUTE OF TECHNOLOGY

Technical Note	LIGO-T2000417-v7-	2021/06/25

NCAL Prototype H1 Surveying Distance Measurement

L. Datrier, E. Daw, M. Hendry, T. Mistry, M. Ross, J. Oberling, J. Kissel

Distribution of this document:

Instrument Science

California Institute of Technology
LIGO Project, MS 100-36
Pasadena, CA 91125
Phone (626) 395-2129
Fax (626) 304-9834
E-mail: info@ligo.caltech.edu

Massachusetts Institute of Technology
LIGO Project, NW22-295
Cambridge, MA 02139
Phone (617) 253-4824
Fax (617) 253-7014
E-mail: info@ligo.mit.edu

LIGO Hanford Observatory
PO Box 159
Richland, WA 99352
Phone (509) 372-8106
Fax (509) 372-8137
E-mail: info@ligo.caltech.edu

LIGO Livingston Observatory
19100 LIGO Lane
Livingston, LA 70754
Phone (225) 686-3100
Fax (225) 686-7189
E-mail: info@ligo.caltech.edu

http://www.ligo.caltech.edu/

Contents

1   Introduction

Gravitational, or "Newtonian," absolute force references ("calibrators") for gravitational wave detectors have been built for all 2nd generation detectors in the global network e.g. [1, 2, 3]. A dominant contribution to uncertainty and potential systematic error in the force from these systems comes the distance between the center of rotation of the calibrator and the detector's test masses (shown, e.g. analytically in [4]). The LIGO NCAL system, [1], was originally designed to use the ratio of its quadrupole and hexapole forces to independently determine this distance to high precision. However, as described in [5], this method relies on knowledge off-axis the location of the NCAL w.r.t. the test mass, and to reduce the estimate's uncertainty to the desired ∼0.1% level relies on impractically long integration time.

In this note we summarize the method used in the final analysis of [1] for determining, $\overrightarrow{TC}$, the three-dimensional vector distance between of the LIGO test mass and the NCAL system's center of rotation, via surveying, CAD model analysis, and vector coordinate transformations. The final results are in the form of numerical evaluated probability distributions of this distance vector, as the raw measured values used (each with uncertainty bounds) must be propagated through non-linear, trigonometric and vector calculations.

The final, numerically evaluated, probability distributions for components of this distance vector, $\overrightarrow{TC}$ are *not* Guassian in character, and *should not be treated as such*. The results presented below are just a human stopping point for sanity checks and conversation. The stopping point is only a part of the whole numerical process of estimating the $2f$ and $3f$ force from the NCAL system described in [1]. However, for the purpose of conversation (and future design consideration), the median of the probability distribution is taken to be the component values, and the upper and lower 1-, 2-, and 3-σ percentile bounds of the distribution are quoted as "uncertainty."

In cartesian coordinates aligned with the LIGO global coordinate system, the components of $\overrightarrow{TC}$ are:

$$\overrightarrow{TC} = 722.8^{+2.48}_{-2.50}\ \hat{x} + 933.0^{+1.54}_{-1.52}\ \hat{y} + 10.0^{+2.98}_{-2.97}\ \hat{z} \tag{1}$$

where dimensions are reported in millimeters, and only the 1-σ upper and lower percentile bounds are shown here for brevity. Section 4 of the document presents histograms of the distributions, and all three 1-, 2-, and 3-σ percentile bounds. Evaluating the answer in terms of polar coordinates, traditionally used in analytic calculations of the force, yields

$$\overrightarrow{TC} = 1180.2^{+2.37}_{-2.38}\ \hat{\rho} + 52.2^{+0.08}_{-0.08}\ \hat{\Phi} + 10.0^{+2.98}_{-2.97}\ \hat{z} \tag{2}$$

where the $\hat{z}$ component is perpendicular to with LIGO global coordinate system's $\hat{x}\hat{y}$ plane (and thus parallel with its $\hat{z}$ direction), and the polar radius $\hat{\rho} = \sqrt{(x^2 + y^2)}$ lies on that plane. Φ is defined in the "+RZ" direction with a right-handed rotation about $\hat{z}$, (i.e. counter-clockwise, if looking down from above the test mass - NCAL system), and $\Phi = 0$ deg is defined from the $-\hat{x}$ direction. $\hat{\rho}$ and $\hat{z}$ values are reported in millimeters, Φ is reported in degrees. See Figure 1 for graphical representation.

This remainder of this document is organized as follows. Section 2 introduces the raw measurements and their uncertainty that have been used to arrive at the numerically evaluated
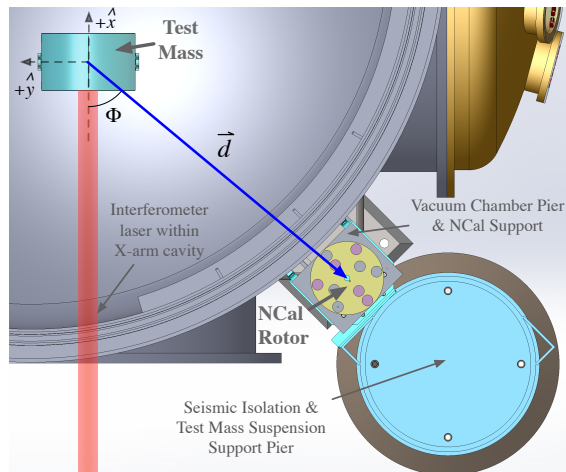
Figure 1: Top-down view of a CAD rendering of the NCal and test mass system. The NCal is shown without its enclosing frame, shell, or motor for clarity. The test mass is shown inside its large vacuum chamber with all suspending elements and other surrounding elements similarly removed. The detector's interferometric laser resonating within the X-arm cavity is shown as it would be, ideally, in full operation. The distance vector, $\vec{d}$, between the NCal center of rotation and Test Mass Center of Mass $\vec{d}$ is indicated in blue, as well as its angle with respect to the $\hat{x}$, interferometer beam, direction – the only component of the NCal force that is measured. While not represented well in this rendering for clarity, in reality, the NCal $\hat{x}\hat{y}$-plane is slightly above of the $\hat{x}\hat{y}$-plane centered on the vertical center of mass of the test mass, and the interferometer beam is not perfectly centered on the front surface.

answer. Section 3 reviews the mathematics needed to convert those raw measurements into the distance vector shown above. Section 4, again, shows the above answer in more complete detail. Section 5 discusses the accuracy and validation of the CAD assembly model of the NCAL system used within this analysis to "measure" the distance between the inaccessible/invisible center of rotation of the NCAL and the accessible/visible external frame of the NCAL system. Finally, Section 6 points to and describes the code used to perform this numerical evaluation.

2 Key Measurements

There exists a constellation of positional references build in to the concrete floor of the experimental hall of the X end-station's vacuum enclosure area (EX VEA), as shown in 2. The X-Y positions of these monuments are known to within ±0.2 mm with respect to the reference of the global interferometer coordinate system origin at the end-station – the "gold standard monument" BTVE-8, set during the initial construction of the facility. There a few other, similar monuments that serve as vertical, Z, position references known to similar accuracy (not shown in Figure 2).
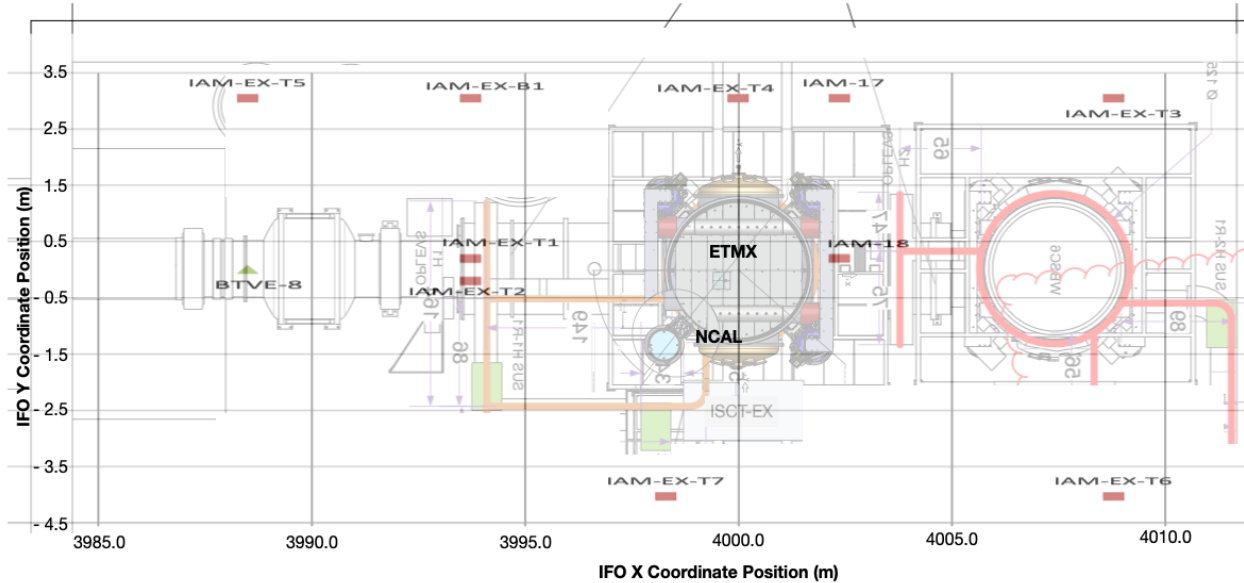
Figure 2: Rough locations of the constellation of global X-Y position monuments in the H1 EXVEA, with respect to the chamber, test mass, and NCAL.

Both the Test Mass and the NCAL positions are measured w.r.t. these monuments referencing the global coordinate system.

Unfortunately, what positions we truly wish to measure, the X, Y, Z position of

- the center of mass of the test mass, and

- the center of rotation of the NCAL in the plane of disc's vertical center of mass

are both enclosed in their respective vacuum or protective chambers and are invisible to surveying equipment. This makes determining a critical parameter in the NCAL force estimate, $\vec{d}$ – the X, Y, and Z (or ρ, Φ, and Z) distance between the test mass CoM and the NCAL center of rotation – a challenge via surveying.

Studies of the position, surveying method, and uncertainty analysis, were all done between Oct 2019 and Oct 2020:

- after the ETMX test mass was replaced (in 2018) and enclosed its vacuum chamber having not been surveyed since its initial installation in 2014.

- when person power and time with the detector were severely limited by the O3 observing run (until Mar 2020), and

- then any potential further measurements limited by the COVID19 pandemic.

As such, we're stuck with interpreting the 2014 surveyed global position of the ETMX test mass, and surveyed global position of the rigid external frame of the NCAL system in its as-built location in X Y and Z. Only three points of a single side of the frame were measured,

because line-of-sight views of the NCAL system after installation are very limited in the crowded EX VEA.

However, from these survey measurements, we use a SolidWorks CAD model of the NCAL system (whose dimensions were verified by physical measurement during construction and assembly of the NCAL system in 2019), and vector coordinate transformation geometry, to propagate the surveyed measurements of the frame (and their uncertainty) to the NCAL's center of rotation. Figure 3 summarizes the order of operations described in this document, wherein we combine several measurements of surveyed positions, in concert with manufacturer's drawings, to determine $\vec{d}$.
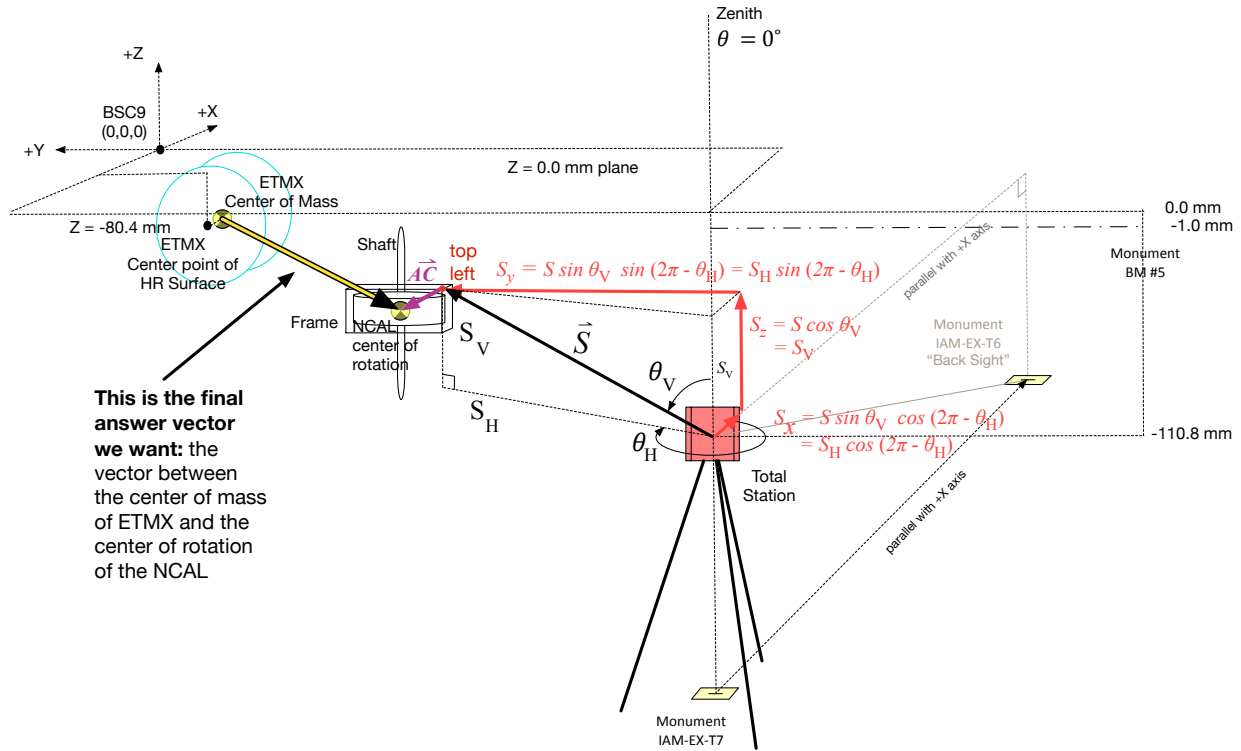

Figure 3: Isometric diagram of the total station's set up with respect to the Test mass and the NCAL.

Because the calculations to produce the NCAL position are non-linear (i.e. they use trigonometric functions and vector algebra), all uncertainties of calculated distance values within the NCAL to Test Mass distance estimate are derived from numerically evaluating the calculation with samples of a distribution of raw input values. All raw input uncertainty has been derived from manufacturer's spec, or educated guess at possible limits of the value, and thus the sampled probability distribution we use to represent them are defined by the central value of the measured position or specified dimension and a uniform (equal) probability of parameter / measurement values between the upper and lower bounds of any raw input to the calculation. Once the numerical evaluation is complete, we characterize posterior distribution using median (50th percentile) as the new calculated answer, and the 1, 2, and 3 σ percentiles (i.e. the 15.9 and 84.1, 2.3 and 97.7, and 0.2 and 99.8 percentiles) as is common practice to arrive at numbers for use in verbal discussion of the answer. It is worth empha-

sizing: all values and uncertainties – from the first, low-level calculations with this these raw input values all the way up to the final force estimates produced by the NCAL system – are numerically evaluated using sampled distributions of input parameters. Any intermediate product's stated value and quoted uncertainty is used only to aide intuition and discussion.

Sub-section 2.1 covers the basic principles of surveying, and how global XYZ coordinates are derived from the instrument's raw measurements. Sub-section 2.2 reports the position of the test mass, and discusses its numerically evaluated uncertainty, given "best guess" assessment of the uncertainty in the 2014 survey of its position. Sub-section 2.3 goes in to more detail about the process of surveying and its uncertainties given that we had more access and more knowledge about the measurement process and reports the results of measuring three points on the rigid frame of the NCAL. Sub-section 2.4 covers the position of the center of rotation w.r.t. to the key external surveyed point on the rigid frame of the NCAL.

2.1 Review of Surveying Technique

In order to survey the position of some new thing within the constellation of monuments at the end-station, one must first set up and establish the position of the total station within that constellation. This is done in a several step process using a 2011 Sokkia Total Station, SET 1X model:

1. Align the tripod of the station over nearest monument to the desired thing. The total station is thus said to "occupy" this monument.

2. Given that tripod sets the total station human height ($\sim$1 m) above the monument, a plum-bob is used ensure the station's XY position is precisely aligned with the cross-hairs scribed into surface of monument (which is flush with the building floor). The quoted precision of this process is ±0.2 mm.

3. The total station, now *positioned* in the XY coordinates, is then *aligned* w.r.t the XY axes of the global coordinate system by defining the horizontal rotation angle, θ_H, where $\theta_H = 0$ is defined to be towards a "back sight" monument, some distance away (in the EXVEA's case, the distance is of order 5-10 m) with the optical scope element within the total station, which has sight-guiding cross-hairs. The uncertainty in this report of angular position is ±1 arcsec, set by the manufacturer's spec matching optical cross-hairs to reported θ_H (see T1100054, under "Angle Measurement," : "Accuracy" : "SET1X model" used on page 8).

4. Finally, The total station's vertical Z position is set w.r.t. a known height monument.

From this point, the X, Y, and Z position, and it's alignment w.r.t. to the horizontal axes is known. The vertical angle, θ_V is defined by local gravity, with $\theta_V = 0°$ at the zenith (straight up).

From this now precisely defined position, one uses another, two-step process to "sight" the desired position of the new thing.

1. The total station is on a 2-axis gimble. After setting the gimble locations for $\theta_V = \theta_H = 0°$, one rotates the total station in the direction of the new thing or position to be measured, and reads off the reported total station values of θ_V and θ_H position with the operator aligning to the new position using the same cross-hairs within an optical scope (similar to θ_H, θ_V also has a manufacturer's spec of ± 1 arcsecond). $+\theta_H$ reads out angles clock-wise from above, and is thus unfortunately a left-handed reading with respect to the $\hat{x}$ direction.

2. Then, an optical prism with finite, well-known dimensions, is used as a retro-reflector (whose contact with the thing / position to be measured has a well-defined relationship to the apparent reflection surface; see details in supporting document T2100262), and held against the point of the thing to be surveyed. With the retro-reflective element aligned back at the total station. The total stations's distance, S, to that new point, is measured via laser Doppler ranging and reported. The uncertainty ± 2 mm, according to the manufacturer's spec (see T1100054, under "Distance Measurement," : "Accuracy" : "With prism Fine Mode" on page 8, which quotes (2 + 2ppm x D) mm, and since D – the distance – is on the order of 10 m or less, we ignore the additional ppm uncertainty that accumulates with distance.)

Armed with S, θ_H, θ_V, (and their uncertainty), one can then use trigonometry to obtain the XYZ position, S_x, S_y, and S_x of the newly measured point.

$$
\begin{aligned}
S_x &= S \sin\theta_V \cos(2\pi - \theta_H) & (3)\\
S_y &= S \sin\theta_V \sin(2\pi - \theta_H) & (4)\\
S_z &= S \cos\theta_V & (5)
\end{aligned}
$$

where θ_H is defined within the trigonometric as $-\theta_H$ or equivalently $2\pi - \theta_H$ because of the position of the NCAL system w.r.t. Total Station in our setup, and because the total station defines $+\theta_H$ in the clockwise-as-viewed-from-above direction.

Of course, if one needs, these XYZ positions are still tied to the occupied monument; to get the relationship between the new surveyed position, $\overrightarrow{P}$, w.r.t. the global IFO origin $\overrightarrow{O}$, one must add the position of the monument,

$$
\overrightarrow{OP} = \overrightarrow{OM} + \overrightarrow{S} \tag{6}
$$

2.2 Test Mass Center of Mass Position

The position of the test mass center of mass, $\overrightarrow{T}$ is reported in the IFO's global coordinate system origin as $\overrightarrow{OT}$, 4 km away, in the center of the vacuum chamber of the Beam Splitter,

$$
\overrightarrow{OT} \equiv \overrightarrow{OM} + \overrightarrow{T} = OT_x\hat{x} + OT_y\hat{y} + OT_z\hat{z} \tag{7}
$$

with the values used for OT_x, OT_y, and OT_z listed in Table 1.

The starting values in arriving at OT_x, OT_y, and OT_z in table 1 are informed by surveying the position of the highly-reflective (HR) "front" surface of the test mass, in-air, w.r.t. to

OT_x [mm]	OT_y [mm]	OT_z [mm]
3999584.9	-200.3	-80.4

Table 1: Components of the position vector between the ETMX center of mass and the origin of the IFO global coordinate system.

the monument constellation at the end station. We collect these starting values from the "actual" column of the 2014 document E1400205, i.e. 3999485.0, -200.3, -80.0 [mm].

However, we augment this position in two ways:

1. propagate the $\hat{x}$ component to the center of mass using the test mass drawing in D0902455 and D080658, which indicate the $\hat{x}$ distance between the HR surface and the center of mass is 99.9 mm, and

2. because the test mass was surveyed in-air, supported by the buoyancy of air, we also decrease the Z position by 0.4 mm as per calculations in T1100616.

The uncertainties in these values are discussed below.

2.2.1   Tess Mass HR Surface Surveying Uncertainty

The procedure for arriving at the results in E1400205 is described in great detail under Section 7 of E1200952, but in short: after the test mass was installed and freely suspended in its final location, the total station was aligned on a monument "in front of" the test mass (occupying IAM-EX-T2 in Figure 2), and

- the longitudinal position of the test mass (along the global X axis) is determined with an optical prism affixed to the surrounding suspension cafe at a known distance away from the test mass HR surface and used as described in Step 2 of Section 2.1.

- the transverse (Y) and vertical (Z) positions were determined by the average of the positions of the left / right and top / bottom bottom of the optic, respectively.

Figure 4 shows a SolidWorks CAD rendering of the retro-reflector used for the measurement, stolen from Figure 4 of E1200952.
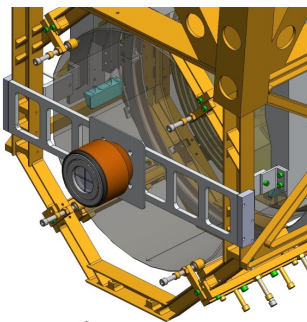

Figure 4: Solidworks assembly of retro-reflector assembly attached to the test mass suspension cage structure.

Unfortunately, due to the invasive nature of the measurement, surveying was not repeated when the test mass replaced in 2018. Any change in position or uncertainty that is missing as a result of this fact is discussed in the context of these values uncertainty below.

E1400205 does not report uncertainty in the test mass position. The "error" column is the difference between the ideal position of the test mass and its measured position, and the "tolerance" indicates how large an error can be tolerated.

The uncertainty in the test mass position is taken to be the "accuracy" stated in the measurement procedure (E1200952):

- $\pm$ 3 mm for the longitudinal direction (global X in this case),

- $\pm$ 1 mm for the transverse (global Y), and

- $\pm$ 1 mm for the vertical (global Z).

Since the derivation of these uncertainties are unclear, we compare these against our intuition as a sanity check. The longitudinal uncertainty is consistent with the manufacturer's spec of ± 2 mm in Doppler ranging, plus, say, an additional 1 mm added to each side of the bound to account for any uncertainty in positioning the retro-reflector on the cage w.r.t. the HR surface. The transverse / vertical uncertainty much larger than "just" the $\pm$ 1 arcsecond manufactorer's spec, at radial distance from the Monument / total station position $\sim$ 6 m away, but we accept the additional uncertainty do to the unknown level of reproduction in the position of the test mass after being replaced.

2.2.2   Tess Mass Thickness Uncertainty

The uncertainty on the distance between the HR surface and the center of mass (99.9 mm), has been taken from the drawings of the test mass, assuming they've been build to spec. Thus, from D080658, we take the larger of the two manufacturing specifications on the assigned thickness, $200^{0.5}_{-1.0}$, and thus assign a ± 1.0 mm uncertainty. We do not divide the uncertainty by 2 (as has been done with the thickness to arrive at the distance between HR surface and CoM) as a conservative allowance for greater uncertainty in the longitudinal position of the CoM.

2.2.3   Tess Mass Vertical Position Adjustment due to Buoyancy Uncertainty

From T1100616, we see that 0.4 mm "sag" is computed from the dynamical model of the quadruple pendulum without uncertainty (see TM Sag in orange in the bottom right of the table in section 4.1). However, we see the corresponding top mass position in the section 4.1 table has both model and measurement via position sensors. Summarizing the discrepancy between model and measurement for all of the suspension types in T1100616, we see that the estimate is consistently 0.05 mm off from the measurement. As such, we would assign the buoyancy a correction of ± 0.05 mm, but chose instead to exclude from all further calculations for simplicity, as it is negligible compared with the 1 mm-level error of the other test mass position uncertainty.

2.2.4 Total Test Mass Position Uncertainty

The total test mass position is numerically evaluated with values of the 2014 surveyed position, the HR surface to CoM projection, and buoyancy correction described above is treated as a uniform ("top-hat", "box-car") distribution of values, where whose central value of the position, or position correction, is that which has been reported. The distribution has equal probability of all values between the central value $\pm$ the quoted uncertainty bound.

Figure 5 shows the distribution of test mass position after numerically evaluting the addition of the 2014 surveyed position of the HR surface, the propagation in the longitudinal direction from the HR surface to the center of mass, and the decrease in vertical position due to the lack of air buoyancy when the test mass is in-vacuum.
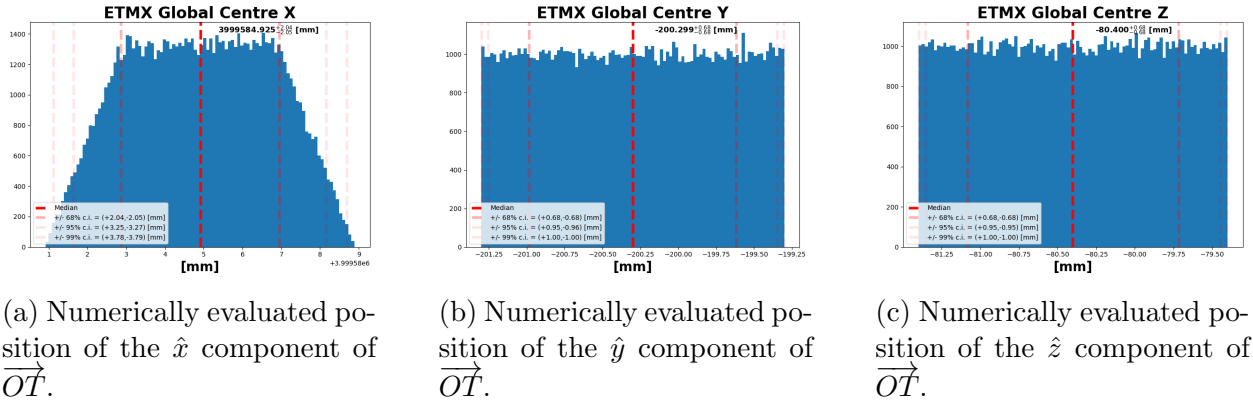

(a) Numerically evaluated position of the $\hat{x}$ component of $\overrightarrow{OT}$.

(b) Numerically evaluated position of the $\hat{y}$ component of $\overrightarrow{OT}$.

(c) Numerically evaluated position of the $\hat{z}$ component of $\overrightarrow{OT}$.

Figure 5: Probability distributions for the test mass position.

As expected, the $\hat{y}$ and $\hat{z}$ components return exactly what has been put in – a uniform distribution, with 3-σ bounds matching the input bounds of $\pm$ 1 mm (recall we assign no uncertainty to the $\hat{z}$ buoyancy correction). However, we immediately see the power of the numerical evaluation in the $\hat{x}$ coordinate, were the sum of two uniform distributions follows the pattern of an Irwin-Hall distribution, with probability (and thus uncertainty) dropping off at the outer limits of the naive bound of the original two bounds added in quadrature.

2.3 NCAL External Frame Position

The position survey of the NCAL's rectangular frame within to the global coordinate system was completed on 22 September 2020 (see LHO aLOG 56801). The technique and instrumentation used is as described in Section 2.1 and with the exact same total station instrument and retro-reflector as in the 2014 survey of the test mass HR surface position. However, because the NCAL prototype does not have a mounting fixture for the optical prism to arrive at the distance from the total station to the NCAL, S, it was merely held over each position by hand. Discussion of potential artifacts and uncertainties that may have arisen from this have been considered and deemed negligible, but are discussed in T2100262.

While a single surveyed point on the frame determines that point's position within the global coordinate system, in order to establish the NCAL frame's *orientation* within the global coordinate system, three positions on the frame were measured, $\overrightarrow{A}$ ("top left"), $\overrightarrow{B}$
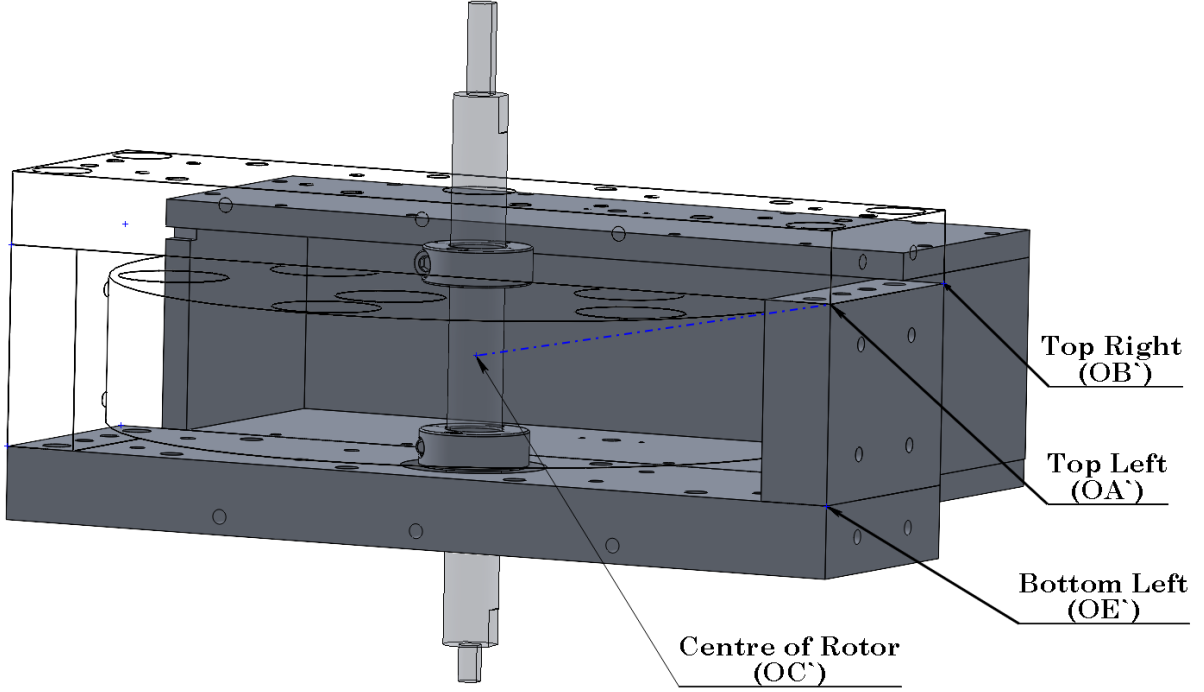
Figure 6: A Solidworks view of the NCAL with labels showing the key points on the NCAL frame. All Solidworks measurements will be denoted with a prime (').

("top right"), and $\overrightarrow{E}$ ("bottom right") with the total station occupying the monument IAM-EX-T7 about 3 m away (see 2). Figure 6 shows where each of these points are on the frame, and Figure 3 shows a cartoon of the measurement of the $\overrightarrow{A}$ point. The relationship between the position as determined from occupying IAM-EX-T7 and the global coordinate system is again determined by adding in the occupied monument's position,

$$\overrightarrow{OA} \equiv \overrightarrow{OM} + \overrightarrow{A} = OA_x\hat{x} + OA_y\hat{y} + OA_z\hat{z} \tag{8}$$

$$\overrightarrow{OB} \equiv \overrightarrow{OM} + \overrightarrow{B} = OB_x\hat{x} + OB_y\hat{y} + OB_z\hat{z} \tag{9}$$

$$\overrightarrow{OE} \equiv \overrightarrow{OM} + \overrightarrow{C} = OE_x\hat{x} + OE_y\hat{y} + OE_z\hat{z} \tag{10}$$

where $\overrightarrow{OM}$ is the set position of the total station at 3998294.5 $\hat{x}$, -4032.0 $\hat{y}$, and -110.8 $\hat{z}$ (where the $\hat{x}$ and $\hat{y}$ position of the total station was set w.r.t. IAM-EX-T7, and the $\hat{z}$ position determined by referencing the height monument BM #5).

The raw values for each measured $\overrightarrow{A}$, $\overrightarrow{B}$, and $\overrightarrow{C}$ are listed in Table 2. The final calculated position in global coordinates of $\overrightarrow{OA}$, $\overrightarrow{OB}$, and , $\overrightarrow{OE}$ are listed in Table 3.

Label	Vector	S [mm]	θ_H	θ_V
Top Left	$\overrightarrow{A}$	2831.3	283° 14' 06" (283.235°)	88° 33' 14" (88.553889°)
Top Right	$\overrightarrow{B}$	2903.6	284° 7' 55" (284.131944°)	88° 34' 22" (88.572778°)
Bottom Left	$\overrightarrow{E}$	2831.0	283° 14' 24" (283.24°)	89° 34' 22" (89.572778°)

Table 2: Raw results from surveying the position of the Top Left, Top Right, and Bottom Left points of the NCAL frame from the monument IAM-EX-T7.

Measurement Label	SolidWorks Label, Oi	Oi_x	Oi_y	Oi_z
Top Left	OA	3998942.5	-1276.8	-39.4
Top Right	OB	3999003.2	-1217.2	-38.5
Bottom Left	OE	3998942.9	-1276.3	-89.7

Table 3: Results from surveying measurements of the frame of the NCAL as mounted on its support structure in the Global coordinate system.

2.3.1 NCAL External Frame Position Uncertainty

For each of the three frame position points, as described in Section 2.1 we assign the raw readings from the total station, θ_H, θ_V, and S the uncertainty from the manufacturer's spec, namely $\pm$ 1 arcsecond for θ_H and θ_V, and $\pm$ 2 mm for S. Figures 7-9 show the uncertainty distributions for each of these positions. The $\hat{y}$ components of each of the positions have the most uncertainty with a 3-σ bound on the distribution at $\sim \pm$ 2 mm.

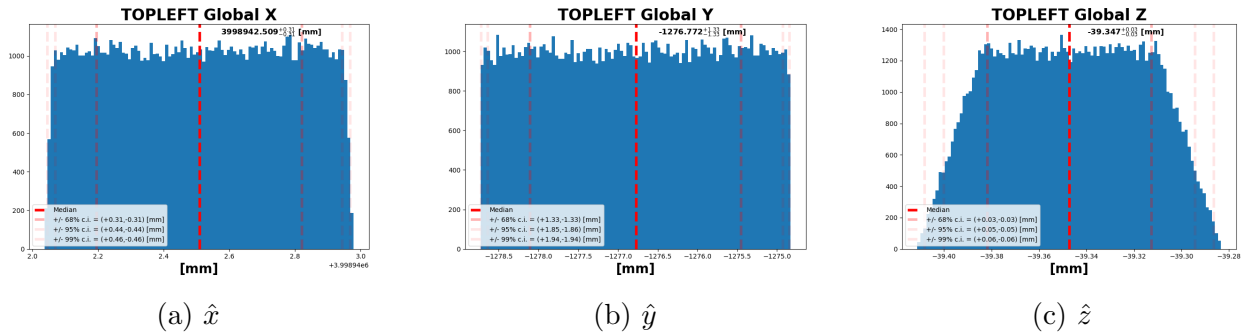(a) $\hat{x}$ (b) $\hat{y}$ (c) $\hat{z}$

Figure 7: Numerically evaluated components of the Top Left position.

2.4 NCAL Center of Rotation w.r.t. its external frame

The NCAL's rotating disk is enclosed within aluminum safety shells and inaccessible within the disk and shaft. As such, we must rely on a CAD model of the NCAL's assembly to
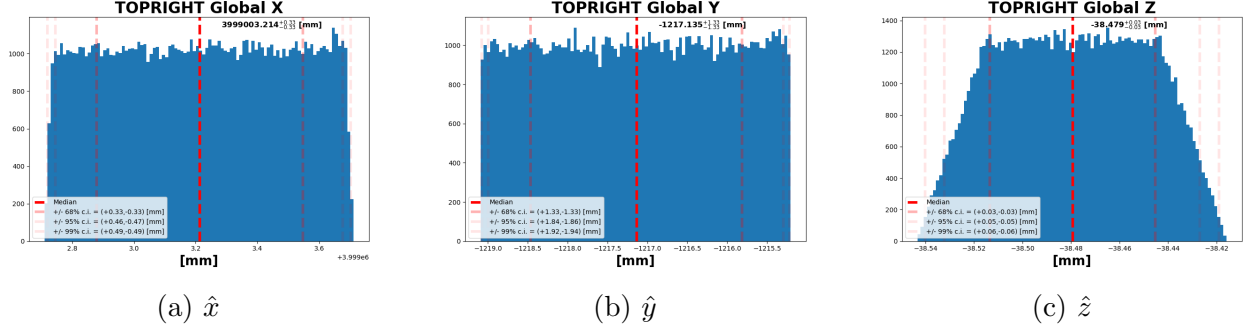
(a) $\hat{x}$ (b) $\hat{y}$ (c) $\hat{z}$

Figure 8: Numerically evaluated components of the Top Right position.

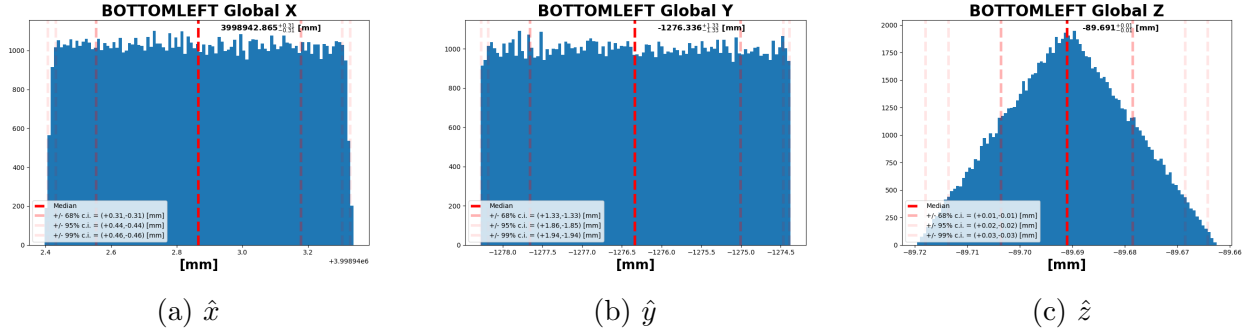(a) $\hat{x}$ (b) $\hat{y}$ (c) $\hat{z}$

Figure 9: Numerically evaluated components of the Bottom Left position.

determine the location of the NCAL's center of rotation with respect to accessible, physically locate-able, parts of the NCAL.

Because we have the as-installed, surveyed positions of the external frame within the global coordinate system, these are the natural connective reference points from which we must "measure" the distance to the center of rotation within the model. While the CAD assembly model is constructed in a Cartesian coordinate system, the relationship between that model's coordinate system and the IFO's global coordinate system using the surveyed measurements from Section 2.3 must still be determined. That mathematical process will be covered later in Section 3, but for now, here, we only describe the distance between the "top left" point of the frame within the model, $\vec{A}'$ – the chosen origin of the CAD assembly – and the center of rotation within the model, $\vec{C}'$.

We define unit vectors within CAD coordinate system as $\hat{n}, \hat{m}$, and $\hat{p}$. $\hat{m}$ and $\hat{p}$ are aligned with $\vec{AB}'$ and $\vec{AE}'$, respectively (the CAD version of the real vectors formed between the "top left" and "top right", and "top left" and "bottom right," surveyed points, again respectively). $\hat{n}$ is then perpendicular to the $\vec{AB}'$ and $\vec{AE}'$ plane. Note, in order to be extra explicit about vectors described in the CAD basis (vs. the same vectors in the IFO global coordinate system), they are marked with the "prime" tick, $'$.

The center of rotation of the NCAL disk w.r.t. to the "top left" point is defined by the vector, $\overrightarrow{AC}'$, and has components,

$$\overrightarrow{AC}' \quad \equiv \quad = \quad AC_n \; \hat{n} + AC_m \; \hat{m} + AC_p \; \hat{p} \tag{11}$$

The values are shown in Figure 10, and listed in 4.

AC_n	AC_m	AC_p
158.75	42.86	31.75

Table 4: Components of $\vec{AC}'$ in $\hat{n}, \hat{m}, \hat{p}$ basis in millimeters.

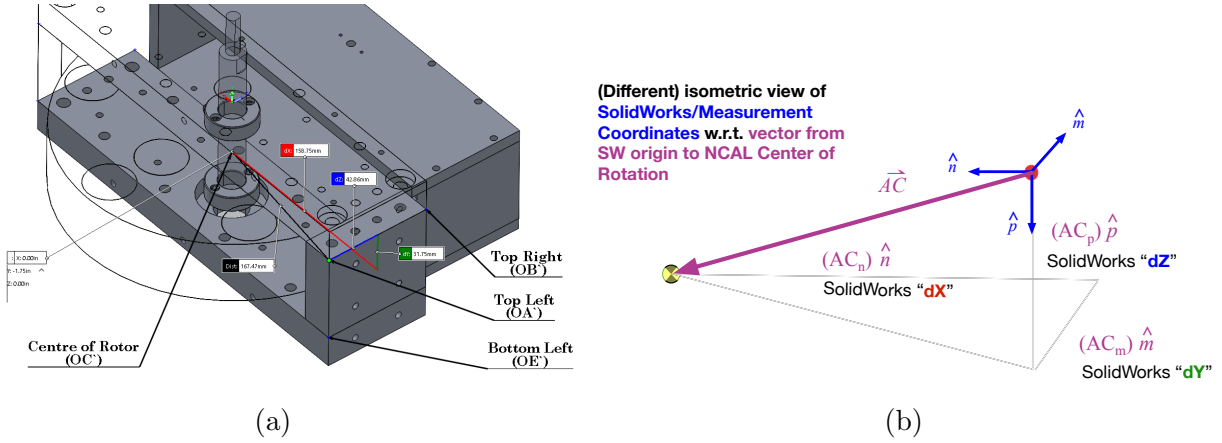
(a)   (b)

Figure 10: (a) SW measurement of $\hat{n}, \hat{m}, \hat{p}$ components of $\vec{AC}'$, marked as dX in red, dZ in blue, and dY in green, respectively and (b) Corresponding map to components of $\vec{AC}'$ in $\hat{n}, \hat{m}, \hat{p}$ basis.

2.4.1 Uncertainty in the Center of Rotation within its frame

The NCal CAD assembly is a concatination of CAD models of the indivudually designed parts. These individual part models are then used to create all machinists drawings. As such, we assume the CAD assembly is exactly as designed with no uncertainty. However, where uncertainty *may* creep in to $\vec{AC}'$ is the *inaccuracy* of the machined parts and physical, as-built, real life assembly, and thus depscrepancy with the SolidWorks model and intended design. As such, prior to installation, the SolidWorks CAD assembly of the NCAL (D1900039) was compared against the real assembly. Discussed in detail in Section 5, we conclude any such discrepancy are an order of magnitude less than those from the uncertainty in surveying, so we include the values in our calculation of the distance without any uncertainty for simplicity.

3   Combining Key Measurements

This section describes how the physical measurements of the frame are used to create an intermediate coordinate system, to which the Solidworks assembly is tied, and from the origin of that intermediate coordinate system, we can have SolidWorks tell us the "rest of the distance" to the center of rotation, and thus arrive at the center of rotation in LIGO's global coordinate system, and in doing so, carrying along the uncertainty of doing so.
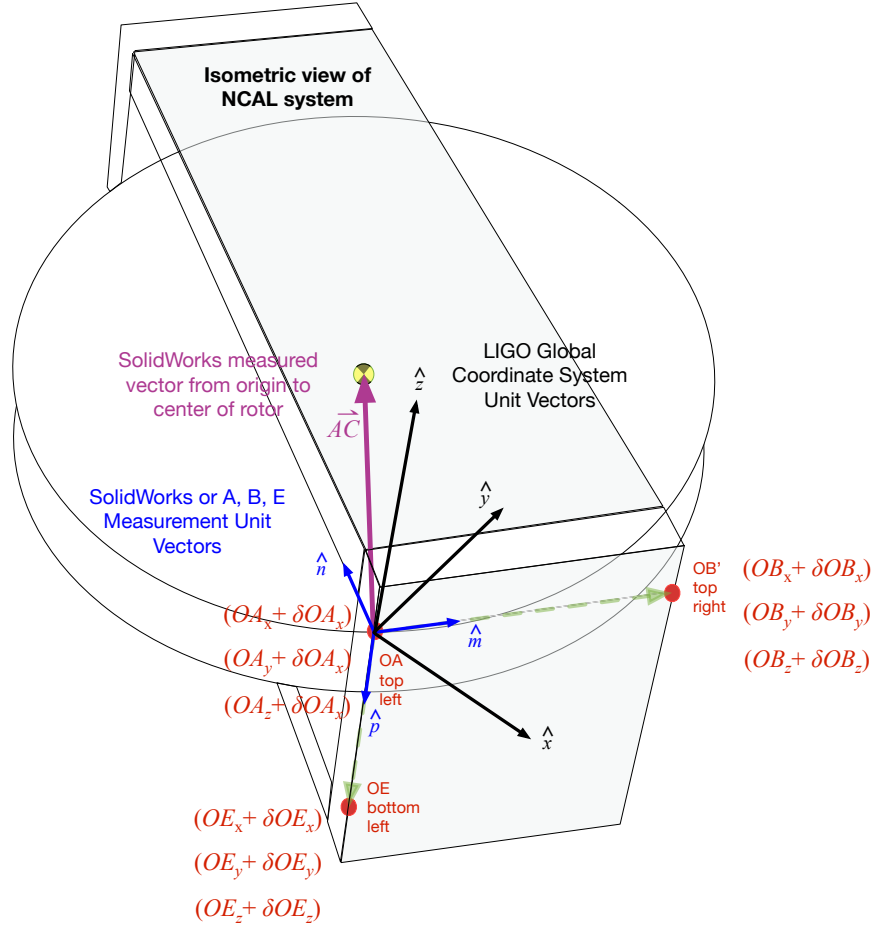

Figure 11: Isometric diagram (with a zoomed in, more top-down, birds-eye view) of the NCAL and the interrelation between the coordinate systems involved in this section.

3.1   Method

First we define the unit-normal coordinate system aligned with LIGO global co-ordinates, such that

$$\hat{x} \equiv \begin{bmatrix} 1 \\ 0 \\ 0 \end{bmatrix} ; \hat{y} \equiv \begin{bmatrix} 0 \\ 1 \\ 0 \end{bmatrix} ; \hat{z} \equiv \begin{bmatrix} 0 \\ 0 \\ 1 \end{bmatrix} ; \tag{12}$$

where:

$$|\hat{x}| = |\hat{y}| = |\hat{z}| = 1 \tag{13}$$

Now, with the measurements described in 2.3 we establish the vectors $\overrightarrow{AB}$ and $\overrightarrow{AE}$ that are located on the NCAL frame, as informed by the top left, top right and bottom left total station measurements:

Top Left to Top Right ($\overrightarrow{AB}$):

$$\overrightarrow{AB} \equiv [OB - OA] \equiv AB_x\hat{x} + AB_y\hat{y} + AB_z\hat{z} \tag{14}$$

Where:

$$AB_x = (OB_x + \delta OB_x) - (OA_x + \delta OA_x) \tag{15a}$$

$$AB_y = (OB_y + \delta OB_y) - (OA_y + \delta OA_y) \tag{15b}$$

$$AB_z = (OB_z + \delta OB_z) - (OA_z + \delta OA_z) \tag{15c}$$

and

$$|\overrightarrow{AB}| = \sqrt{(AB_x + \delta AB_x)^2 + (AB_y + \delta AB_y)^2 + (AB_z + \delta AB_z)^2} \tag{16a}$$

$$|\overrightarrow{AB}| = \left\{ \left([OB_x + \delta OB_x] - [OA_x + \delta OA_x]\right)^2 \right.$$
$$+ \left([OB_y + \delta OB_y] - [OA_y + \delta OA_y]\right)^2$$
$$\left. + \left([OB_z + \delta OB_z] - [OA_z + \delta OA_z]\right)^2 \right\}^{1/2} . \tag{16b}$$

Top Left to Bottom Left ($\overrightarrow{AE}$):

$$\overrightarrow{AE} \equiv [OE - OA] \equiv AE_x\hat{x} + AE_y\hat{y} + AE_z\hat{z} \tag{17}$$

Where:

$$AE_x = (OE_x + \delta OE_x) - (OA_x + \delta OA_x) \tag{18a}$$

$$AE_y = (OE_y + \delta OE_y) - (OA_y + \delta OA_y) \tag{18b}$$

$$AE_z = (OE_z + \delta OE_z) - (OA_z + \delta OA_z) \tag{18c}$$

and:

$$|\overrightarrow{AE}| = \sqrt{(AE_x + \delta AE_x)^2 + (AE_y + \delta AE_y)^2 + (AE_z + \delta AE_z)^2} \tag{19a}$$

$$|\overrightarrow{AB}| = \left\{ \left([OE_x + \delta OE_x] - [OA_x + \delta OA_x]\right)^2 \right.$$
$$+ \left([OE_y + \delta OE_y] - [OA_y + \delta OA_y]\right)^2$$
$$\left. + \left([OE_z + \delta OE_z] - [OA_z + \delta OA_z]\right)^2 \right\}^{1/2} . \tag{19b}$$

Note that a representative uncertainty term in the measured values of each component, δOA_i (etc) are carried around in the mathematical formalism to help convey where and how each uncertainty will appear. However, as mentioned in Section 2, when all is said, what's done is a numerical evaluation, sampling from the distribution of calculated frame positions.

With these vectors $\overrightarrow{AB}$ and $\overrightarrow{AE}$, we can create an orthonormal basis set of unit vectors that can be directly, one-to-one, mapped on to the SolidWorks model using $\overrightarrow{AB}$, $\overrightarrow{AE}$, and their cross-product – insisting that the origin of the SolidWorks coordinate system is the top-left point in both OA and OA'), and that the frame piece along which $\overrightarrow{AB}$ and $\overrightarrow{AE}$ lie is square and the vectors are perpendicular such that $\overrightarrow{AB} = \overrightarrow{AB}'$ and $\overrightarrow{AE} = \overrightarrow{AE}'$.

Define $\hat{m}$ in terms of $\hat{x}, \hat{y}, \hat{z}$ components of $\overrightarrow{AB}$:

$$\hat{m} \equiv \frac{\overrightarrow{AB}}{|\overrightarrow{AB}|} = m_x\,\hat{x} + m_y\,\hat{y} + m_z\,\hat{z} \tag{20}$$

$$= \frac{AB_x}{|\overrightarrow{AB}|}\,\hat{x} + \frac{AB_y}{|\overrightarrow{AB}|}\,\hat{y} + \frac{AB_z}{|\overrightarrow{AB}|}\,\hat{z} \tag{21}$$

$$\hat{m} = \frac{(OB_x + \delta OB_x) - (OA_x + \delta OA_x)}{|\overrightarrow{AB}|}\,\hat{x}$$
$$+ \frac{(OB_y + \delta OB_y) - (OA_y + \delta OA_y)}{|\overrightarrow{AB}|}\,\hat{y}$$
$$+ \frac{(OB_z + \delta OB_z) - (OA_z + \delta OA_z)}{|\overrightarrow{AB}|}\,\hat{z} \tag{22}$$

Define $\hat{p}$ in terms of $\hat{x}, \hat{y}, \hat{z}$ components of $\overrightarrow{AE}$:

$$\hat{p} \equiv \frac{\overrightarrow{AE}}{|\overrightarrow{AE}|} = p_x\,\hat{x} + p_y\,\hat{y} + p_z\,\hat{z} \tag{23}$$

$$= \frac{AE_x}{|\overrightarrow{AE}|}\,\hat{x} + \frac{AE_y}{|\overrightarrow{AE}|}\,\hat{y} + \frac{AE_z}{|\overrightarrow{AE}|}\,\hat{z} \tag{24}$$

$$\hat{p} = \frac{(OE_x + \delta OE_x) - (OA_x + \delta OA_x)}{|\overrightarrow{AE}|}\,\hat{x}$$
$$+ \frac{(OE_y + \delta OE_y) - (OA_y + \delta OA_y)}{|\overrightarrow{AE}|}\,\hat{y}$$
$$+ \frac{(OE_z + \delta OE_z) - (OA_z + \delta OA_z)}{|\overrightarrow{AE}|}\,\hat{z} \tag{25}$$

Define $\hat{n}$ from $\hat{m}$ and $\hat{p}$:

$$\hat{n} \equiv \hat{m} \times \hat{p} = n_x\,\hat{x} + n_y\,\hat{y} + n_z\,\hat{z} \tag{26}$$

$$= \det \begin{vmatrix} \hat{x} & \hat{y} & \hat{z} \\ m_x & m_y & m_z \\ p_x & p_y & p_z \end{vmatrix} \tag{27}$$

$$= \det \begin{vmatrix} m_y & m_z \\ p_y & p_z \end{vmatrix} \hat{x} + \det \begin{vmatrix} m_x & m_z \\ p_x & p_z \end{vmatrix} \hat{y} + \det \begin{vmatrix} m_x & m_y \\ p_x & p_y \end{vmatrix} \hat{z} \tag{28}$$

$$= + (m_y p_z - m_z p_y)\,\hat{x} - (m_x p_z - m_z p_x)\,\hat{y} + (m_x p_y - m_y p_x)\,\hat{z} \tag{29}$$

$$\begin{aligned}
\hat{n} = \;&+ \Bigg[\frac{1}{|AB|}\frac{1}{|AE|} \Big(\big[(OB_y + \delta OB_y) - (OA_y + \delta OA_y)\big]\big[(OE_z + \delta OE_z) - (OA_z + \delta OA_z)\big] \\
&\quad - \big[(OB_z + \delta OB_z) - (OA_z + \delta OA_z)\big]\big[(OE_y + \delta OE_y) - (OA_y + \delta OA_y)\big] \Big) \Bigg]\, \hat{x} \\
&- \Bigg[\frac{1}{|AB|}\frac{1}{|AE|} \Big(\big[(OB_x + \delta OB_x) - (OA_x + \delta OA_x)\big]\big[(OE_z + \delta OE_z) - (OA_z + \delta OA_z)\big] \\
&\quad - \big[(OB_z + \delta OB_z) - (OA_z + \delta OA_z)\big]\big[(OE_x + \delta OE_x) - (OA_x + \delta OA_x)\big] \Big) \Bigg]\, \hat{y} \\
&+ \Bigg[\frac{1}{|AB|}\frac{1}{|AE|} \Big(\big[(OB_x + \delta OB_x) - (OA_x + \delta OA_x)\big]\big[(OE_y + \delta OE_y) - (OA_y + \delta OA_y)\big] \\
&\quad - \big[(OB_y + \delta OB_y) - (OA_y + \delta OA_y)\big]\big[(OE_x + \delta OE_x) - (OA_x + \delta OA_x)\big] \Big) \Bigg]\, \hat{z}
\end{aligned} \tag{30}$$

With the definition of the SolidWorks coordinate system in terms of the measured external frame positions in LIGO global coordinate system, we can map the components of the SolidWorks vector between the $\hat{n}, \hat{m}, \hat{p}$ basis and the center of rotation, $\overrightarrow{AC'}$, and incorporate the uncertainty from the frame measurement. Figure 12a shows the vector $\overrightarrow{AC}$ in each coordinate system, and Figure 12b shows the projection (dot product) of each each $\hat{n}$, $\hat{m}$, and $\hat{p}$ basis vector on to each $\hat{x}$, $\hat{y}$, and $\hat{z}$ basis vector, and/or defines the nine angles θ_x, θ_y, θ_z, ψ_x, ψ_y, ψ_z, ϕ_x, ϕ_y, ϕ_z in between each basis vector.

With these definitions, we can project the values of $\overrightarrow{AC'}$ in the $\hat{n}$, $\hat{n}$, $\hat{p}$ basis we have from Section 2.4 in to the $\hat{x}$, $\hat{y}$, $\hat{z}$ basis – or, in other words, create the vector $\overrightarrow{OC}$, the vector from the IFO global coordinate system origin to the center of rotation – and we've correctly included the uncertainty in doing so. The following five systems of equations are all equivalent
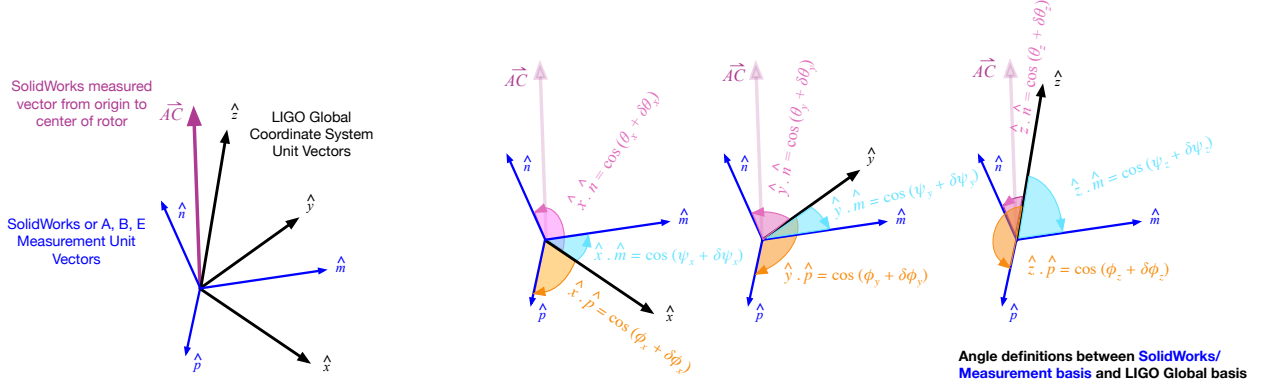
(a) Both coordinate systems $\hat{n}, \hat{m}, \hat{p}$ shown with $\overrightarrow{AC}$.

(b) Projections and angles between in $\hat{n}, \hat{m}, \hat{p}$ basis and $\hat{x}, \hat{y}, \hat{z}$ basis.

Figure 12: Definition of relationships between SolidWorks coordinate basis vectors, $\hat{n}, \hat{m}, \hat{p}$ and LIGO global coordinate basis vectors $\hat{x}, \hat{y}, \hat{z}$

expressions for the projections.

$$
\begin{aligned}
OC_x &= AC_n \cos\theta_x + AC_m \cos\psi_x + AC_p \cos\phi_x \\
OC_y &= AC_n \cos\theta_y + AC_m \cos\psi_y + AC_p \cos\phi_y \\
OC_z &= AC_n \cos\theta_z + AC_m \cos\psi_z + AC_p \cos\phi_z
\end{aligned} \tag{31}
$$

$$
\overrightarrow{OC} = \mathbf{M}\,\overrightarrow{AC} \tag{32}
$$

$$
\begin{bmatrix} OC_x \\ OC_y \\ OC_z \end{bmatrix} =
\begin{bmatrix} \hat{x}\cdot\hat{n} & \hat{x}\cdot\hat{m} & \hat{x}\cdot\hat{p} \\ \hat{y}\cdot\hat{n} & \hat{y}\cdot\hat{m} & \hat{y}\cdot\hat{p} \\ \hat{z}\cdot\hat{n} & \hat{z}\cdot\hat{m} & \hat{z}\cdot\hat{p} \end{bmatrix}
\begin{bmatrix} AC_n \\ AC_m \\ AC_p \end{bmatrix} \tag{33}
$$

$$
\begin{aligned}
OC_x &= (\hat{x}\cdot\hat{n})\,AC_n + (\hat{x}\cdot\hat{m})\,AC_m + (\hat{x}\cdot\hat{m})\,AC_p \\
OC_y &= (\hat{y}\cdot\hat{n})\,AC_n + (\hat{y}\cdot\hat{m})\,AC_m + (\hat{y}\cdot\hat{p})\,AC_p \\
OC_z &= (\hat{z}\cdot\hat{n})\,AC_n + (\hat{z}\cdot\hat{m})\,AC_m + (\hat{z}\cdot\hat{p})\,AC_p
\end{aligned} \tag{34}
$$

$$
\begin{aligned}
OC_x &= n_x\,AC_n + m_x\,AC_m + p_x\,AC_p \\
OC_y &= n_y\,AC_n + m_y\,AC_m + p_y\,AC_p \\
OC_z &= n_z\,AC_n + m_z\,AC_m + p_z\,AC_p
\end{aligned} \tag{35}
$$

where from Eq. 35 it's clear that we can just multiply the components of $\overrightarrow{AC'}$ by the correct $\hat{x}$, $\hat{y}$, $\hat{z}$ components from Eqs. 22, 25, and 30 of $\hat{m}$, $\hat{n}$, $\hat{p}$, basis to arrive at projection of $\overrightarrow{AC'}$ in to $\overrightarrow{OC}$. But most importantly the uncertainty of each surveyed frame point's physical position OA, OB, and OE is baked in.

3.2   NCAL Center of Rotation in LIGO Global Coordinates

The NCAL's Center of Rotation, as calculated by combining the surveyed position of the frame (Section 2.3) and the CAD assembly "measured" distance from the frame to the center of rotation results (Section 2.4) using the methods described in Section 3.1 are listed in Table 5. The uncertainty (confidence intervals on the distributions of component values) are shown in Figure 13.

Label	OC_x	OC_y	OC_z
NCAL Center of Rotation	3998862.1	-1133.3	-70.4

Table 5: Calculated values of the NCAL center of rotation in the LIGO global coordinate system as projected from SolidWorks Assembly and surveyed positions of the external frame.
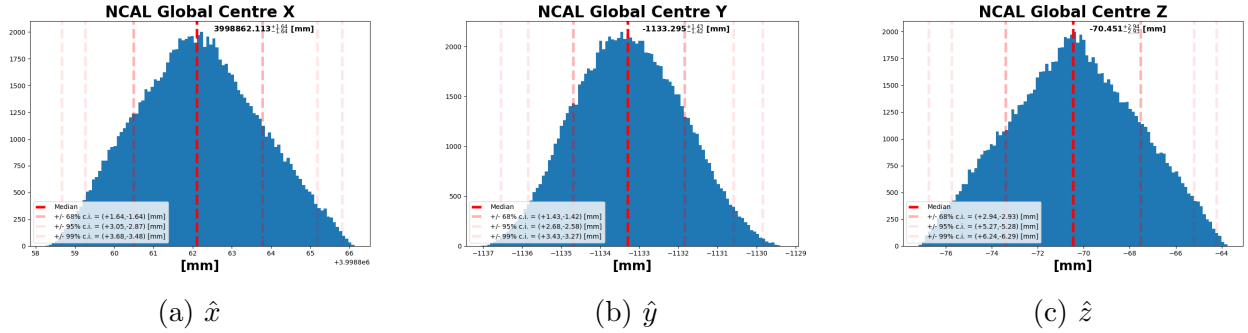

(a) $\hat{x}$ (b) $\hat{y}$ (c) $\hat{z}$

Figure 13: Numerically evaluated components of the NCAL's center of rotation.

4   Results

Now we get the final answer by subtracting the vector between the test mass $\overrightarrow{OT}$ (Section 2.2) from the center of rotation of the NCAL $\overrightarrow{OC}$ (Section 3.2),

$$\overrightarrow{TC} \equiv \overrightarrow{OC} - \overrightarrow{OT} \tag{36}$$

As the LIGO global coordinate system's origin subtracts away, we report the answer both in terms of $\hat{x}$, $\hat{y}$, and $\hat{z}$ which are still aligned within the global coordinate system (see Table 6 and Figure 14), but we also report the answer in terms more natural for the analytic expressions for the force estimate, i.e. cylindrical coordinates, with magnitudes rho, Φ, and (a repeat of) z (see Table 7 and Figure 15), Also, since this is the "final answer" we report the uncertainty on these values in terms of 1-, 2-, and 3-σ confidence intervals of the numerically evaluated distribution.

Label	Median	1-σ c.i.	2-σ c.i.	3-σ c.i.
TC_x	-722.8	$+2.48$ -2.5	$+4.66$ -4.59	$+6.20$ -5.99
TC_y	-933.0	$+1.54$ -1.52	$+2.91$ -2.81	$+3.89$ -3.78
TC_z	+10.0	$+2.98$ -2.97	$+5.38$ -5.39	$+6.63$ -6.66

Table 6: Calculated median, and 1-, 2-, and 3-σ, percentile values for the calculated probability distribution of each Cartesian component of the distance vector between the center of mass of the ETMX test mass and the NCAL center of rotation, $\vec{TC}$. The Cartesian, $\hat{x}\hat{y}\hat{z}$, components are aligned with LIGO global coordinate system. All values are reported in millimeters.

Label	Median	1-σ c.i.	2-σ c.i.	3-σ c.i.
TC_ρ	+1180.2	$+2.37$ -2.38	$+4.46$ -4.52	$+5.93$ -6.09
TC_Φ	+52.2	$+0.08$ -0.08	$+0.15$ -0.15	$+0.20$ -0.19
TC_z	+10.0	$+2.98$ -2.97	$+5.38$ -5.39	$+6.63$ -6.66

Table 7: Calculated median, and 1-, 2-, and 3-σ, percentile values for the calculated probability distribution of each component of the distance vector between the center of mass of the ETMX test mass and the NCAL center of rotation, $\vec{TC}$, in polar-cylindrical coordinates. The $\hat{z}$ component is perpendicular to with LIGO global coordinate system's $\hat{x}\hat{y}$ plane, and the polar coordinates lie on that plane. $\hat{rho}$ and $\hat{z}$ values are reported in millimeters. Φ is reported in degrees, and is defined in the +RZ direction with a right-handed rotation about $\hat{z}$, (i.e. counter-clockwise, if looking down from above the test mass - NCAL system), and $\Phi = 0$ deg is defined by the $-\hat{x}$ direction.
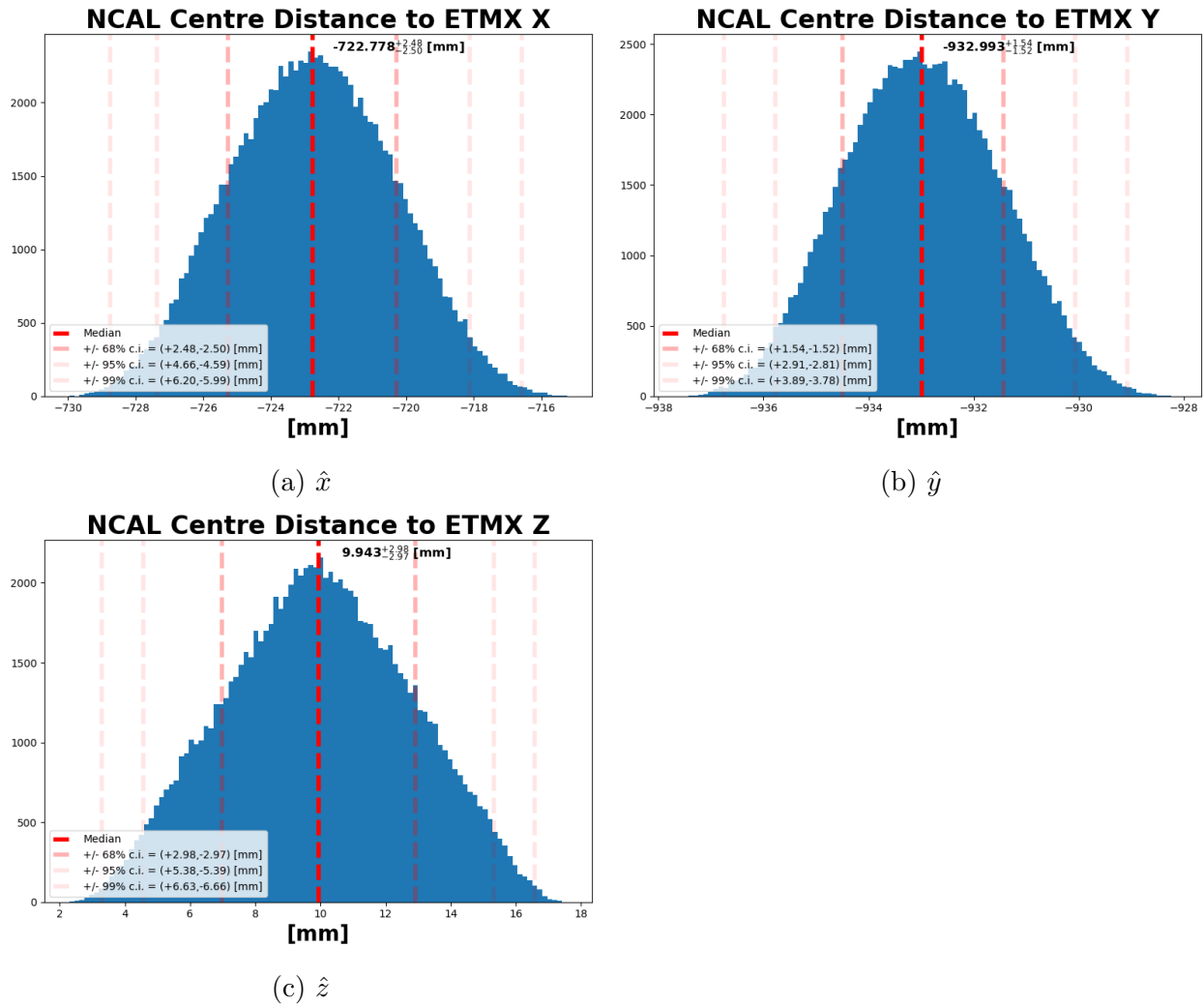
(a) $\hat{x}$

(b) $\hat{y}$

(c) $\hat{z}$

Figure 14: Numerically evaluated components of the NCAL's center of rotation in cartesian coordinates.
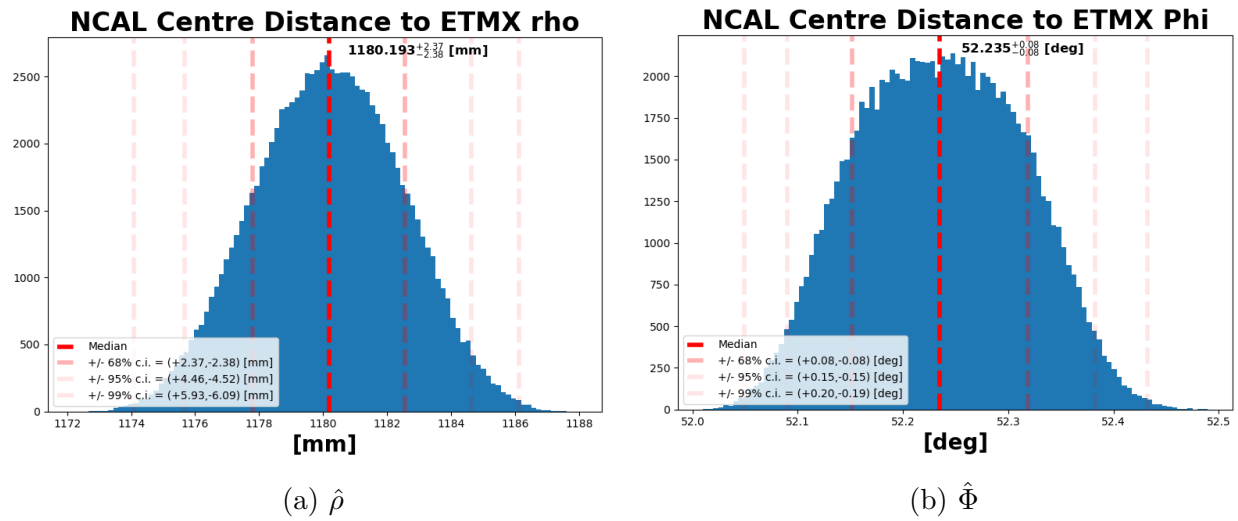
(a) $\hat{\rho}$

(b) $\hat{\Phi}$

Figure 15: Numerically evaluated components of the NCAL's center of rotation in cylindrical coordinates (the $\hat{z}$ distribution is identical in both coordinate systems, so only one is shown for brevity).

5 Corroboration of NCAL SolidWorks Assembly

The $\hat{n} - \hat{m}$ position of the rotor's center of rotation with respect to the frame is defined by the shaft's alignment through the rotor, the holes in the top and bottom frame, and the perpendicularity of the frame. All holes within the as-built rotor were verified to be within ± 5 μm of the design location via coordinate measuring machine. The 0.75 inch shaft is press-fit through the 0.75 inch hole in the center of the rotor. The through-holes within the top/bottom frame, in which the 1 inch bearings are pressed, and the bolt-holes which define the placement and perpendicularity of the frame were all machined at standard CNC machine tolerance of ± 0.127 mm (0.005 inches). The perpendicularity is defined by the mating of cut surfaces of the frames, all connected as flush with no evidence of error.

As such, we assume the $\hat{n} - \hat{m}$ of the center of the rotor w.r.t. the frame within the SolidWorks Model (determined by computing the center of the cylindrical surface formed by the outer edge of the rotor) has uncertainty no larger than the tolerance at which each parts were machined, i.e. ± 0.127 mm (0.005 inches).

The $\hat{p}$ position is the most uncertain, as it relies on the assembled vertical position of the shaft/rotor within the frame holes, which may be set relatively freely within the 0.5 inch range of motion that is left between the 2 inch thick rotor mated to its 0.25 inch thick base plate and the 2.75 inch height of the frame cavity. On the real assembly, the position was aligned to have the upper and lower surfaces of the rotor/base plate equidistant from the frame. The "gap" between the upper surface of the rotor and the lower surface of the top frame plate was then roughly confirmed using height stand / dial indiciator system to be at 0.23 ± 0.05 inches $= 5.842 \pm 1.27$ mm which consistent with the design value of 0.25 inches $= 6.35$ mm (see details of this measurement discussed in G2101300). As such, the SolidWorks assembly is forced to ensure this gap is 0.25 inches, and thus the $\hat{p}$ position of the center of the rotor w.r.t. frame is set, and we assume machine-tolerance uncertainty of ± 0.127 mm (0.005 inches).

Since we attribute ± 0.127 mm to all $\hat{n}, \hat{m}, \hat{p}$ components, and these are an order of magnitude less than those from surveying, we include the values in our calculation of the distance without any uncertainty for simplicity.

6 Analysis Code

All analysis reported in this document has been calculated and produced using the python script, `final_results_plots.py`, which is a wrapper around a python library of modules, called `NCal_SurveyPosition.py`, from which `final_results_plots.py` performs the following operations on 10^5 iterations of the following process:

- the input parameter values and uncertainty bounds described in Section 2 are initiated by calling the values hard-coded in the `NCal_SurveyPosition.py` module `hc_params` whose definition starts on line 455,

- those parameters, and their uncertainty bounds, are turned in to probability distributions with the `NCal_SurveyPosition.py` module `distribution_sample` whose defini-

tion starts on line 119,

- each of the three surveyed positions of the NCAL frame (now each a sample from the distribution of S, θ_H, θ_V distances and angles from monument IAM-EX-T7 to the frame) are converted in to the vectors $\overrightarrow{OA}, \overrightarrow{OB}$, and $\overrightarrow{OE}$ in LIGO global Cartesian $\hat{x}, \hat{y}, \hat{z}$ coordinates with the `NCal_SurveyPosition.py` module `totalstation_to_cartesian` whose definition starts on line 66 (running the sampled values from $\overrightarrow{A}, \overrightarrow{B}$, and $\overrightarrow{E}$ in Table 2 through Eqs. 3-5 and adding in the monument position $\overrightarrow{OM}$,

- The $\hat{x}, \hat{y}$, and $\hat{z}$ components of the $\hat{n}, \hat{m}, \hat{p}$ basis are computed using the LIGO global coordinates of the measured frame positions in the `NCal_SurveyPosition.py` module `compute_new_basis` whose definiton starts on line 193 (following Eqs. 22, 25, and 30),

- The SolidWorks "measured" vector, $\overrightarrow{AC'}$ in the $\hat{n}, \hat{m}, \hat{p}$ is projected on to the $\hat{x}, \hat{y}, \hat{z}$ basis and added the Top Left position, $\overrightarrow{OA}$, to establish the NCAL center of rotation, $\overrightarrow{OC}$ in the `NCal_SurveyPosition.py` module `compute_centre` whose definition starts on line 278 (following Eq. 35),

- The test mass center of mass is computed from adding the test mass thickness (as a sampled distribution with bounds $+/-$ 1 mm) to $\hat{x}$ coordinate of the surveyed "center of the HR surface" position (as a sampled distribution with $\hat{x}, \hat{y}, \hat{z}$ bounds of $+/-$ 3, 1, 1 mm), and 0.4 mm buoyancy correction is subtracted from the $\hat{z}$ coordinate of the "center of the HR surface" position creating $\overrightarrow{OT}$ (a la discussion in 2.2), in line, without the need for any module (i.e. just as discussed in Subsection 2.2 and Eq. 7), and

- The test mass center of mass, $\overrightarrow{OT}$, is subtracted from the NCAL center of rotation, $\overrightarrow{OC}$, to form the final answer – the distance between the two, $\overrightarrow{TC}$ – in either Cartesian or Cylindrical coordinates using the `NCal_SurveyPosition.py` module `compute_distance` whose definition starts on line 337 (following Eq. 36).

The histograms of all of the above distributions of each of these steps are what's shown throughout Sections 2 - 4 are produced with the `NCal_SurveyPosition.py` module `PNG_hist` whose definition starts on line 378.

An independent Matlab script which quickly performs a virtually identical numerical evaluation but with much less sophistication, polish, and computational overhead, called coordinateCalc.m has been used as a cross-check of the results. It produces results consistent with `final_results_plots.py`.

7 Related Documents

LIGO DCC Document ID	Title	Description
E1400205	IAS LHO primary optic as built alignment summary.	Position of HR surface of ETMX.
D0902455	ETM Subtrate Assembly	Longitudinal distance between ETMX HR Surface and ETMX COM
D1100291	aLIGO IAS LHO Monuments.	Map and list of global-coordinate position monuments. including those used at X-end-station.
D0901153	ALIGO AdvLIGO BSC9-H1 XYZ local CS for ETMX.	SolidWorks Rendering used for sanity checks only.
LHO aLOG 56801	Survey Measurements for NCAL Prototype	Position of Frame Measurement Points w.r.t. End-station Monuments
D1900039	NCAL SolidWorks Assembly	Position of NCAL Center of Rotation w.r.t. Frame
D1900280	NCAL chamber drawing.	Solidworks Rendering used for sanity checks only.

References

[1] Ross M P, Mistry T, Datrier L, Kissel J *et al.* 2021, in preparation *Phys. Rev. D*

[2] Inoue Y, Haino S, Kanda N, Ogawa Y, Suzuki T, Tomaru T, Yamanmoto T and Yokozawa T 2018 *Phys. Rev. D* **98**(2) 022005 URL https://link.aps.org/doi/10.1103/PhysRevD.98.022005

[3] Estevez D, Lieunard B, Marion F, Mours B, Rolland L and Verkindt D 2018 *Classical and Quantum Gravity* **35** 235009 URL https://doi.org/10.1088%2F1361-6382%2Faae95f

[4] Datrier L, Kissel J, Mistry T and Ross M 2020 *LIGO DCC* URL https://dcc.ligo.org/LIGO-T2000238

[5] MPRoss, Kissel J, Datrier L and Mistry T 2021 *LIGO DCC* URL https://dcc.ligo.org/LIGO-T2100066